Paper 47

©Civil-Comp Press, 2012
Proceedings of the Eleventh International Conference
on Computational Structures Technology,
B.H.V. Topping, (Editor),
Civil-Comp Press, Stirlingshire, Scotland

Large Deformation Analysis of Laminated Composite Plates

T. Yıldız[1], Y. Olcay[2] and H. Darendeliler[1]
[1] Department of Mechanical Engineering
Middle East Technical University, Ankara, Turkey
[2] STM Defense Technologies Engineering and Trade Incorporated
Ankara, Turkey

Abstract

The objective of this paper is to investigate the behaviour of laminated fibre-reinforced composite plates subject to large deformations by developing a shell finite element and to predict the failure by illustrating the critical elements of the model. The laminates are assumed to be orthotropic and the first order shear deformation theory is applied in the formulation by using triangular shell elements. Laminates under transverse loading were analysed for different boundary conditions and ply orientations. The maximum stress, Hashin's and Tsai-Wu failure criteria are integrated to the code to detect first ply failure.

Keywords: laminated composite plate, finite element analysis, large deformation, nonlinear analysis, first order plate theory, first ply failure.

1 Introduction

Composites are advanced engineering materials with superior mechanical properties that can be tailored and diversified among the purpose of application. The requirements of the design are accomplished by the combination of two or more distinct materials on macroscopic scale in order to improve the desired properties like strength, stiffness, corrosion resistance, fatigue life, weight, attractiveness, thermal insulation or conductivity. Their high strength-to-weight ratio exceeding that of the constituents is the main attribute which makes mechanics of composite materials a more popular area of interest. The primary usage of advanced composite materials is for aerospace applications. Aircraft are distinguished from the other vehicles by the fact that structural factors of safety are low and power-to-weight ratios are high. These levels are achieved by using materials with high specific material properties and precise design procedures. Airplanes, rockets missiles and various structural components of these, including engines and also satellite applications have been routinely produced with glass, carbon and kevlar composites [1-4].

The most crucial issue in the design of the composites arises from the fact that, directionally dependent properties make the analysis and design applications more difficult. In order for the design to be reliable, damage modes, which are dependent on loading, stacking sequence and specimen geometry must be predicted. There are many theories to predict the onset of failures and their progression. Most of the failure criteria are based on the stress state in the lamina. An accurate kinematic model of the laminate is necessary to determine the stress and strain fields which are the key parameters of the design to be controlled [5].

Limit analyses are generally recovered by the use of Mises-like theories, especially with Tsai-Wu criterion, which is the adaptation of failure envelopes used in isotropic elasticity to anisotropy. While the investigation of damage onset is generally carried out with maximum stress, Tsai-Wu, Tsai-Hill, Azzi-Tsai theories or in some cases with the modified or combined versions of these popular criteria, the property degradation and the ultimate collapse of the laminates are determined by the implementation of the mathematical model into a finite element solver.

The formulation generated by Padhi, Shenoi, Moy and Hawkins [6] is one of the few studies dealing with progressive failure of laminated plates under transverse loading. In the study, failure is predicted by employing different failure criteria, geometric nonlinearity is considered and first order plate theory is applied by using a commercial finite element program. Parhi, Bhattacharyya and Sinha [7] indicated the first ply failure of the composite plates by the direct implementation of Tsai-Wu criteria to their model. Spottswood and Palazotto [8] worked on the initial and progressive failure of the curved composite panel designed to resist transverse loading through the use of Hashin failure criterion. In the analysis, geometric nonlinearity which allows large displacements but small to moderate rotations is considered. In the study of Prusty, Satsangi and Ray [9], first ply failure analysis of laminated panels under transverse loading was carried out with Yeh-Stratton criterion to determine the failure loads together with the well known theories maximum stress, maximum strain, Tsai-Wu, Tsai-Hill and Hoffman. Lin and Hu [10] introduced a mixed failure criterion which was composed of Tsai-Wu and maximum stress theories. This criterion was used to determine the failure onset and the proposed degrading model was used to represent post-damage mode of the composite laminates under biaxial tensile loads. The progressive failure analysis of laminated composite plates has been performed in linear and elastic range by Pal and Ray [11] and Pal and Bhattacharyya [12]. Under transverse static loading, after estimating the failure onset, the related stiffness of the failed lamina had been discarded completely, i.e., the model was degraded according to the failure mode of the weakest layer. After a ply-by-ply analysis, ultimate failure load of the laminate was achieved. Huang [13] applied bridging model technique to characterize nonlinearity of composites undergoing inelastic deformation. In the study, the compliance matrix is constructed as a combination of fibre and matrix materials instead of the treating the structure with the unified properties of the two constituents. The results were given for several composite beams subjected to 3-point bending.

In the present study, a finite element program is developed to analyze the nonlinear behaviour of the laminated composite plates under transverse loading. The deformed forms of the laminates having various combinations of ply orientations are plotted until the first ply failure. The initiation of the damage is detected through three different failure theories; maximum stress, Hashin's and Tsai-Wu failure criteria, which are integrated to the developed code.

2 Governing equations

The flat shell finite element, which was developed for elastic-plastic analysis of homogenous materials in a previous study [14], is adapted to composite materials. The deformation and motion of a body of volume V_o and surface area A_o in the undeformed state can be defined by $x_i = x_i(X_1, X_2, X_3, t)$ where x_i is the Eulerian or spatial coordinates and X_i is the Lagrangian or material coordinates. The virtual work equation for a virtual displacement δx is given as

$$\int_{V_o} S_{ij} \delta E_{ij} dV_o = \int_{A_o} t_k \delta x_k dA_o \tag{1}$$

In the equation above, S_{ij} is the second Piola-Kirchoff stress tensor, E_{ij} is the Lagrangian strain tensor, t_k is the traction vector at a spatial point referred to the undeformed configuration. The material time derivative of Equation (1) gives

$$\int_{V_o} \left(\dot{S}_{ij} \delta E_{ij} + S_{ij} \delta \dot{E}_{ij}\right) dV_o = \int_{A_o} \dot{t}_k \delta x_k dA_o \tag{2}$$

Imposing the well-known equations

$$E_{ij} = \frac{1}{2}\left(\frac{\partial x_k}{\partial X_i}\frac{\partial x_k}{\partial X_j} - \delta_{ij}\right) \tag{3}$$

$$S_{ij} = \frac{\rho_o}{\rho}\frac{\partial X_i}{\partial x_k}\sigma_{kl}\frac{\partial X_j}{\partial x_k} \tag{4}$$

where ρ and ρ_0 are the densities in deformed and reference configurations respectively, and σ_{kl} is the Cauchy stress tensor, the following equation can be obtained from Equation (2)

$$\int_{V_o} \frac{\rho_o}{\rho}\left(\bar{\sigma}_{kl}\frac{\partial \delta v_k}{\partial x_l} + \sigma_{ml}\frac{\partial v_k}{\partial x_l}\frac{\partial \delta v_k}{\partial x_m}\right) dV_o = \int_{A_0} \dot{t}_k \delta x_k dA_o \tag{5}$$

where $\bar{\sigma}_{kl}$ is the Truesdell stress rate and v_k is the velocity. The velocity gradient can be written in terms of its symmetric and skew-symmetric parts, D_{kl}, the rate of deformation tensor and W_{kl}, the spin tensor, respectively as

$$\frac{\partial v_k}{\partial x_l} = D_{kl} + W_{kl} \tag{6}$$

$\bar{\sigma}_{kl}$ can be obtained using the mentioned property of the velocity gradient through the existence of the Jaumann rate of Cauchy stress tensor, σ_{kl}^{*}

$$\bar{\sigma}_{kl} = \sigma_{kl}^{*} + \frac{\partial v_m}{\partial x_m}\sigma_{kl} - \sigma_{km}D_{lm} - \sigma_{ml}D_{km} \tag{7}$$

Imposing Equation (7) into Equation (5) gives

$$\int_{V_o} \frac{\rho_o}{\rho}\left[\left(\sigma_{kl}^{*} + \frac{\partial v_m}{\partial x_m}\sigma_{kl}\right)\delta D_{kl} - 2\sigma_{ml}D_{km}\delta D_{kl} + \sigma_{ml}\frac{\partial v_k}{\partial x_l}\frac{\partial \delta v_k}{\partial x_m}\right] dV_o = \int_{A_0} \dot{t}_k \delta v_k dA_o \tag{8}$$

In the updated Lagrangian formulation the Cauchy and Kirchoff stress tensors σ_{kl} and τ_{kl} are related as

$$\tau_{kl} = \frac{\rho_o}{\rho}\sigma_{kl} \tag{9}$$

and their rates give the following equation

$$\tau_{kl}^{*} = \sigma_{kl}^{*} + \frac{\partial v_m}{\partial x_m}\sigma_{kl} \tag{10}$$

Assuming $\rho_o/\rho \approx 1$ and $\partial v_m/\partial x_m \ll 1$ for incompressible materials, the following equation can be written

$$\tau_{kl}^{*} = C_{klmn}D_{mn} \tag{11}$$

where C_{klmn} is the constitutive relation. Equation (8) finally becomes

$$\int_V \left(C_{klmn}D_{mn}\delta D_{kl} - 2\sigma_{ml}D_{km}\delta D_{kl} + \sigma_{ml}\frac{\partial v_k}{\partial x_l}\frac{\partial \delta v_k}{\partial x_m}\right) dV = \int_A \dot{t}_k \delta v_k dA \tag{12}$$

In the above equation V and A are the volume and surface area of the body at time *t*. The rate of deformation tensor D_{ij} and gradients of velocity tensor $v_{i,j}$ can be written as vectors $\boldsymbol{d}$ and $\boldsymbol{w}$, respectively, whereas the forth order tensor C_{ijpq} can be expressed as a matrix $\boldsymbol{C}$. Then Equation (12) gives

$$\int_V (\delta \boldsymbol{d}^T \boldsymbol{C}\boldsymbol{d} - 2\delta \boldsymbol{d}^T \widehat{\boldsymbol{\sigma}}\boldsymbol{d} + \delta \boldsymbol{w}^T \widetilde{\boldsymbol{\sigma}}\boldsymbol{w}) dV = \int_A \delta \boldsymbol{v}^T \dot{\boldsymbol{t}} dA \tag{13}$$

where

$$\boldsymbol{d}^T = [D_{11} \quad D_{22} \quad 2D_{12} \quad 2D_{23} \quad 2D_{31}] \tag{14}$$

$$\boldsymbol{w}^T = [v_{1,1} \quad v_{1,2} \quad v_{1,3} \quad v_{2,1} \quad v_{2,2} \quad v_{2,3} \quad v_{3,1} \quad v_{3,2}] \tag{15}$$

and $\widehat{\boldsymbol{\sigma}}$ and $\widetilde{\boldsymbol{\sigma}}$ are appropriately formed stress matrices.

3 The layered flat shell finite element

The shear deformable theory of Mindlin is used in the formulation of the layered flat shell finite element. The velocity field of the shell element whose midsurface coincides with the xy-plane can be written as

$$\begin{aligned} v_1(x_1,x_2,x_3,t) &= v_1^0(x_1,x_2,t) + x_3\dot{\psi}_2(x_1,x_2,t) \\ v_2(x_1,x_2,x_3,t) &= v_2^0(x_1,x_2,t) - x_3\dot{\psi}_1(x_1,x_2,t) \\ v_3(x_1,x_2,x_3,t) &= v_3^0(x_1,x_2,t) \end{aligned} \tag{16}$$

where v_i are the velocities in the corresponding x_i directions, v_i^0 are the associated midsurface velocities $(i = 1,2,3)$, $\dot{\psi}_1$ and $\dot{\psi}_2$ are the rate of change of normal rotations in the x_2x_3 and x_1x_3 planes, respectively, and t is the time. Then by using Equations (14) and (15) the vectors $\boldsymbol{d}$ and $\boldsymbol{w}$ can be expressed as

$$\boldsymbol{d} = \begin{bmatrix} v_{1,1}^0 + x_3\dot{\psi}_{2,1} \\ v_{2,2}^0 - x_3\dot{\psi}_{1,2} \\ v_{1,2}^0 + v_{2,1}^0 + x_3(\dot{\psi}_{2,2} - \dot{\psi}_{1,1}) \\ v_{3,2}^0 - \dot{\psi}_1 \\ v_{3,1}^0 + \dot{\psi}_2 \end{bmatrix} \tag{17}$$

$$\boldsymbol{w} = \begin{bmatrix} v_{1,1}^0 + x_3\dot{\psi}_{2,1} \\ v_{1,2}^0 + x_3\dot{\psi}_{2,2} \\ \dot{\psi}_2 \\ v_{2,1}^0 + x_3\dot{\psi}_{1,1} \\ v_{2,2}^0 + x_3\dot{\psi}_{1,2} \\ -\dot{\psi}_1 \\ v_{3,1}^0 \\ v_{3,2}^0 \end{bmatrix} \tag{18}$$

The anisotropic interpolation functions suggested by Tessler and Hughes [15] are employed to develop an effective and simple Mindlin element, and to prevent shear locking. Then v_m^0 and $\dot{\psi}_\alpha (\alpha = 1,2)$ can be expressed in terms of the nodal variables of a three node element as

$$v_1^0 = \xi_i {}^i v_1^0$$
$$v_2^0 = \xi_i {}^i v_2^0$$
$$v_3^0 = \xi_i {}^i v_3^0 + \frac{1}{2}\left(b_j \xi_k \xi_i - b_k \xi_i \xi_j\right) {}^i\dot{\psi}_1 + \frac{1}{2}\left(a_j \xi_k \xi_i - a_k \xi_i \xi_j\right) {}^i\dot{\psi}_2 \tag{19}$$
$$\dot{\psi}_1 = \xi_i {}^i\dot{\psi}_1$$
$$\dot{\psi}_2 = \xi_i {}^i\dot{\psi}_2$$

where ξ_i are the triangular area coordinates, $a_i = x_{1k} - x_{1j}$ and $b_i = x_{2j} - x_{2k}$ and the permutation $i = 1,2,3;\ j = 2,3,1; k = 3,1,2$. Defining the element degrees of freedom vector $\boldsymbol{q}$ as

$$\boldsymbol{q} = \begin{bmatrix} {}^1v_1^0 & {}^1v_2^0 & {}^1v_3^0 & {}^1\dot{\psi}_1 & {}^1\dot{\psi}_2 & {}^2v_1^0 & \dots & {}^3\dot{\psi}_2 \end{bmatrix} \tag{20}$$

In the above equation, the node number is indicated by a left superscript. Then the vectors $\boldsymbol{d}, \boldsymbol{w}$ and $\boldsymbol{v}$ can be expressed in terms of element degrees of freedom

$$\boldsymbol{d} = \boldsymbol{HBq} \tag{21}$$

$$\boldsymbol{w} = \boldsymbol{GRq} \tag{22}$$

$$\boldsymbol{v} = \boldsymbol{Nq} \tag{23}$$

where the matrices $\boldsymbol{H}$ and $\boldsymbol{G}$ are the functions of x_3 only, the matrices $\boldsymbol{B}$ and $\boldsymbol{R}$ are formed to express $\boldsymbol{d}$ and $\boldsymbol{w}$ in terms of elements degrees of freedom and $\boldsymbol{N}$ is the shape function matrix. Finally Equation (13) gives

$$\int_V \left(\delta\boldsymbol{q}^T\boldsymbol{B}^T\underline{\boldsymbol{C}}\boldsymbol{B}\boldsymbol{q} - 2\delta\boldsymbol{q}^T\boldsymbol{B}^T\underline{\hat{\boldsymbol{\sigma}}}\boldsymbol{B}\boldsymbol{d} + \delta\boldsymbol{q}^T\boldsymbol{R}^T\underline{\tilde{\boldsymbol{\sigma}}}\boldsymbol{R}\boldsymbol{w}\right)dV = \int_A \delta\boldsymbol{q}^T\boldsymbol{N}^T\dot{\boldsymbol{t}}dA \tag{24}$$

where

$$\underline{\boldsymbol{C}} = \sum_{n=1}^{L}\int_{h_n}^{h_{n+1}} \boldsymbol{H}^T\boldsymbol{C}\,\boldsymbol{H}dx_3 \tag{25}$$

$$\underline{\hat{\boldsymbol{\sigma}}} = \sum_{n=1}^{L}\int_{h_n}^{h_{n+1}} \boldsymbol{H}^T\hat{\boldsymbol{\sigma}}\,\boldsymbol{H}dx_3 \tag{26}$$

$$\underline{\tilde{\boldsymbol{\sigma}}} = \sum_{n=1}^{L}\int_{h_n}^{h_{n+1}} \boldsymbol{G}^T\,\tilde{\boldsymbol{\sigma}}\boldsymbol{G}dx_3 \tag{27}$$

In the above equations L is the number of layers and h_n is the distance between the midsurface of the plate and the bottom of the n^{th} layer.

4 Constitutive equations

The stress-strain relations for an orthotropic material in material coordinates $x_1^m,\ x_2^m,\ x_3^m$ can be written in matrix form as follows [10, 16-18]:

$$\begin{bmatrix}\sigma_1\\ \sigma_2\\ \sigma_6\\ \sigma_4\\ \sigma_5\end{bmatrix}=\begin{bmatrix}Q_{11} & Q_{12} & 0 & 0 & 0\\ Q_{12} & Q_{22} & 0 & 0 & 0\\ 0 & 0 & Q_{66} & 0 & 0\\ 0 & 0 & 0 & k^2Q_{44} & 0\\ 0 & 0 & 0 & 0 & k^2Q_{55}\end{bmatrix}\begin{bmatrix}\varepsilon_1\\ \varepsilon_2\\ \varepsilon_6\\ \varepsilon_4\\ \varepsilon_5\end{bmatrix} \tag{28}$$

where k^2 is the shear correction factor which is taken as $5/6$ [16-20]. The normal stress in the thickness direction is neglected. The reduced stiffnesses Q_{ij} are given by

$$\begin{gathered}Q_{11}=\frac{E_1}{1-\nu_{12}\nu_{21}}\\ Q_{22}=\frac{E_2}{1-\nu_{12}\nu_{21}}\\ Q_{12}=\frac{\nu_{12}E_2}{1-\nu_{12}\nu_{21}}\\ Q_{44}=G_{23}\\ Q_{55}=G_{13}\\ Q_{66}=G_{12}\end{gathered} \tag{29}$$

The stress-strain relation can be defined in local coordinates x_1, x_2, x_3 by introducing the transformed reduced stiffness matrix $\bar{\boldsymbol{Q}}=\boldsymbol{T}^T\boldsymbol{Q}\boldsymbol{T}$

$$\begin{bmatrix}\sigma_{11}\\ \sigma_{22}\\ \sigma_{12}\\ \sigma_{23}\\ \sigma_{13}\end{bmatrix}=\begin{bmatrix}\bar{Q}_{11} & \bar{Q}_{12} & \bar{Q}_{16} & 0 & 0\\ \bar{Q}_{12} & \bar{Q}_{22} & \bar{Q}_{26} & 0 & 0\\ \bar{Q}_{16} & \bar{Q}_{26} & \bar{Q}_{66} & 0 & 0\\ 0 & 0 & 0 & \bar{Q}_{44} & \bar{Q}_{45}\\ 0 & 0 & 0 & \bar{Q}_{45} & \bar{Q}_{55}\end{bmatrix}\begin{bmatrix}\epsilon_{11}\\ \epsilon_{22}\\ \epsilon_{12}\\ \epsilon_{23}\\ \epsilon_{13}\end{bmatrix} \tag{30}$$

In the transformation matrix $\boldsymbol{T}$ given below the angle between the x_1-axis and x_1^m-axis is defined by θ.

$$\boldsymbol{T}=\begin{bmatrix}cos^2\theta & sin^2\theta & -2\sin\theta\cos\theta & 0 & 0\\ sin^2\theta & cos^2\theta & 2\sin\theta\cos\theta & 0 & 0\\ \sin\theta\cos\theta & -\sin\theta\cos\theta & cos^2\theta-sin^2\theta & 0 & 0\\ 0 & 0 & 0 & \cos\theta & \sin\theta\\ 0 & 0 & 0 & -\sin\theta & \cos\theta\end{bmatrix} \tag{31}$$

5 Results

To observe the large deformation behaviour of laminated composites, the structures are loaded until the prediction of the first ply failure by using the maximum stress, Hashin's and Tsai-Wu criteria.

Several plates constructed of glass/epoxy are considered with different fiber angles and boundary conditions. Material properties used in the analysis are given in Table 1. In the finite element analyses a mesh with 600 three noded triangular elements and 341 nodes is used for all cases. Deformed shapes of 2.8 mm thick 14-layered symmetric laminates having in-plane dimensions of 300 mm × 100 mm are depicted for the stacking sequences of $[0/90/0/90/0/90/0]_s$, $[15/-15/15/-15/15/-15/15]_s$, $[30/-30/30/-30/30/-30/30]_s$, $[45/-45/45/-45/45/-45/45]_s$ and $[60/-60/60/-60/60/-60/60]_s$. First ply failure loads are determined for each laminate, and load-deflection characteristics are compared.

$E_1 = 139400\ MPa$	$X_T = 1537.2\ MPa$
$E_2 = 7650\ MPa$	$X_C = 1722.4\ MPa$
$E_3 = 4350\ MPa$	$Y_T = Z_T = 42.7\ MPa$
$G_{12} = G_{13} = 4350\ MPa$	$Y_C = Z_C = 42.7\ MPa$
$G_{23} = 1020\ MPa$	$R = 79.7\ MPa$
$v_{12} = v_{13} = 0.29$	$S = T = 102.4\ MPa$
$v_{23} = 0.49$	$t = 0.2\ mm/ply$

Table 1 Material properties of graphite/epoxy material

Starting with Figure 1; it is noticed that first ply failure loads are highest for $[15/-15/\ldots]_s$ laminated plate and decrease with increasing ply angles seeing the minimum at $[60/-60/\ldots]_s$ plate, except the plate with $[0/90/\ldots]_s$ stacking sequence for one end clamped case. Moreover the highest and lowest first ply failure loads are obtained, respectively, by maximum stress and Tsai-Wu criteria where Hashin's criterion results lie in between. The $[0/90/\ldots]_s$ plate displays moderate first ply failure strength since it includes both 0° and 90° plies. As the ply angle increases the load carried by the matrix increases and matrix failure becomes dominant. Considering that the matrix strength values are quite low, early failure at 90° plies is expected. On the other hand; the fiber strength values are extremely high and 0° plies fail at considerably high load levels. Similar behaviors are observed for the clamped roller and both ends clamped cases which are given in Figure 2 and 3, respectively. For all the end conditions; the difference between the maximum and minimum first ply failure loads that have been obtained for different ply angles, are significant. Thus; it can be concluded that first ply failure loads are decreasing with increasing ply angles except $[0/90/\ldots]_s$ plate which shows an average first ply failure load compared to other stacking sequences and also first ply failure loads obtained by the maximum stress, Hashin's and Tsai Wu criteria are in decreasing order.

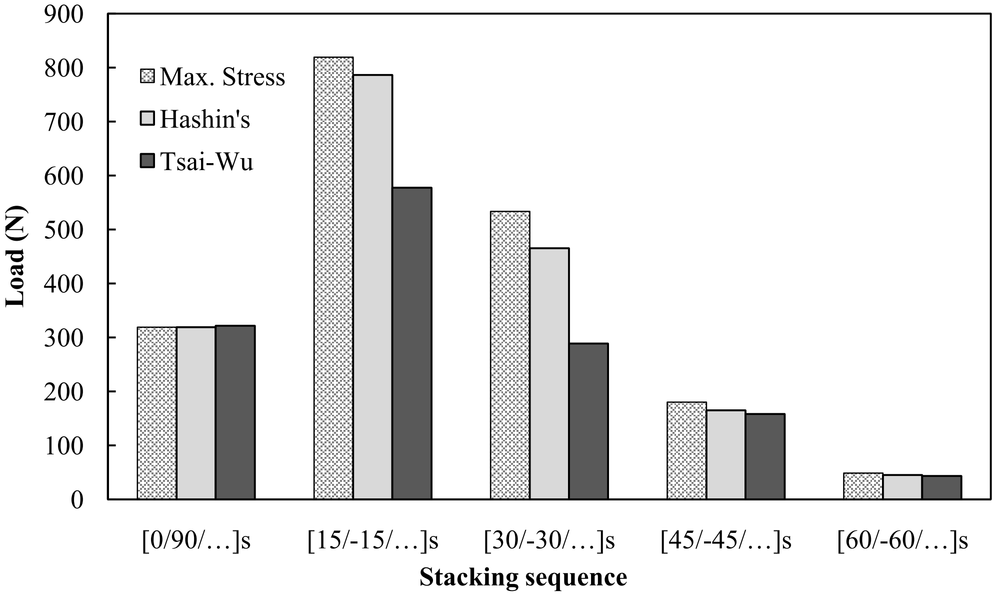

Figure 1: First ply failure loads of one end clamped plates

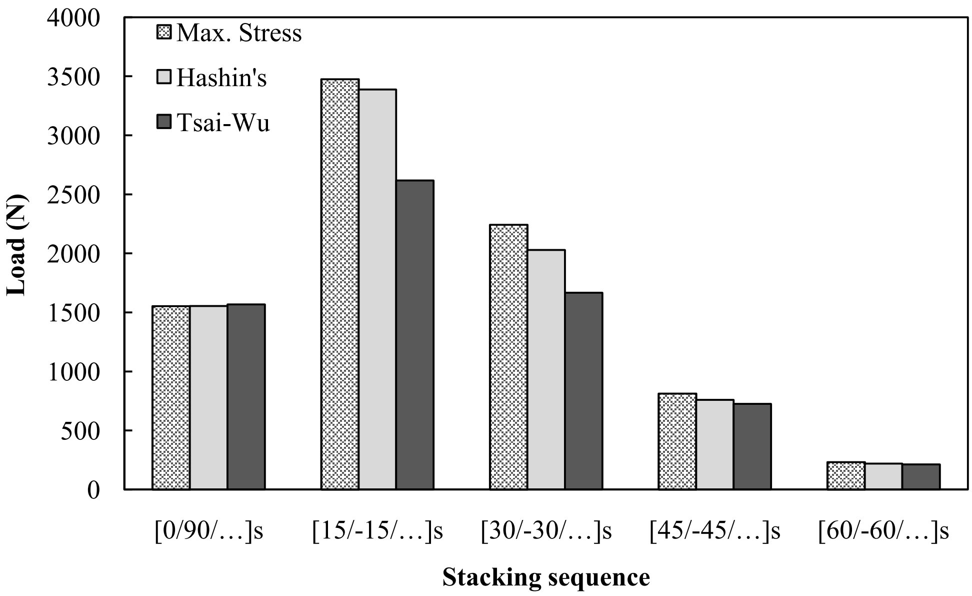

Figure 2: First ply failure loads of clamped roller plates

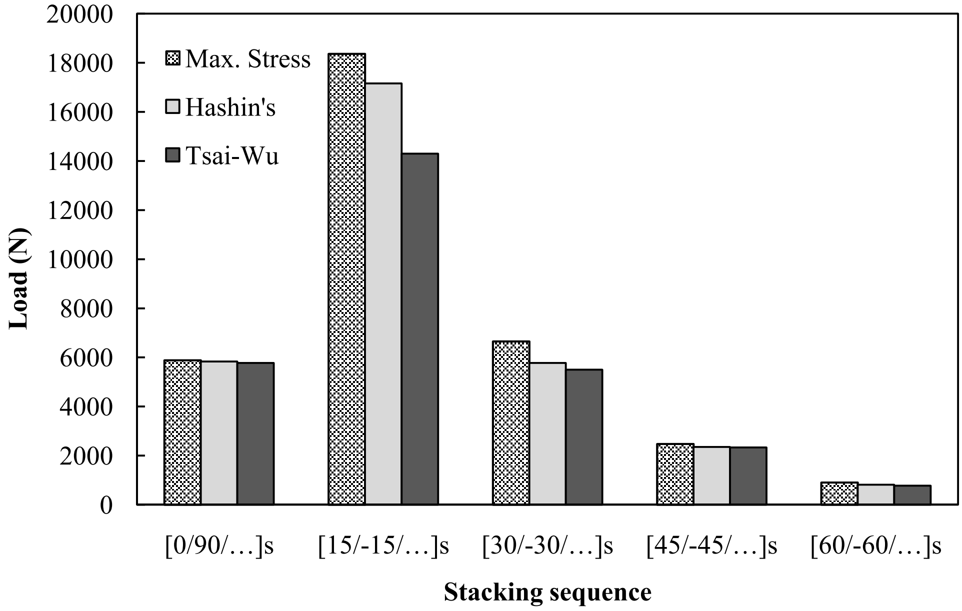

Figure 3: First ply failure loads of both ends clamped plates

Reviewing Figures 4, 5 and 6, it is seen that the maximum midsurface deflection values that have been observed at the first ply failure decrease with respect to increasing ply angles. Also, the maximum midsurface displacement values obtained at first ply failure load by maximum stress criterion are the highest; the smallest values are calculated by Tsai Wu criterion, whereas the values found by Hashin's criterion are in between. Noting the maximum midsurface deflections for [0/90/…]s plate; it can be said that, the resulting maximum displacement values determined by the three failure criteria are almost equal for each end condition. The maximum midsurface displacement results follow a similar trend with the first ply failure loads in terms of ply angles and failure criteria for all end conditions.

Although three different failure theories are considered to determine the first ply failure loads and maximum midsurface displacements for all laminates by the developed code, the related deflection plots are depicted in Figures 7, 8 and 9 only for the maximum allowable loads obtained by the Tsai-Wu criterion. As seen in Figure 7, the largest and smallest midsurface deflections are obtained, respectively, for $[15/-15/\ldots]_s$ and $[60/-60/\ldots]_s$ plates for one end clamped cases. The maximum tip deflection is as high as 164 mm which is almost 55% of the beam span. The minimum tip deflection is 130 mm and the difference between the maximum and minimum deflections, considering all ply angles, is about 10% of the beam length. The same tendencies are observed for clamped roller and both end clamped plates although the maximum deflection values found are about 10 % and 3 % of the beam span for these cases, respectively.

It is also observed that, although considerably large differences found for first ply failure loads determined at different ply angles, the variation for maximum midsurface deflections is about 10 % considering each end condition.

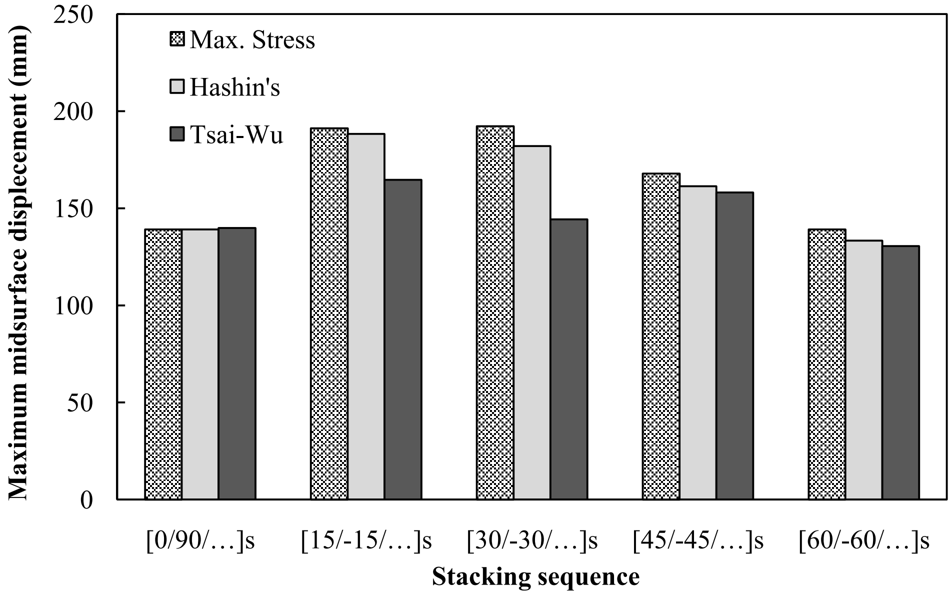

Figure 4: Maximum tip displacement at first ply failure for one end clamped plates

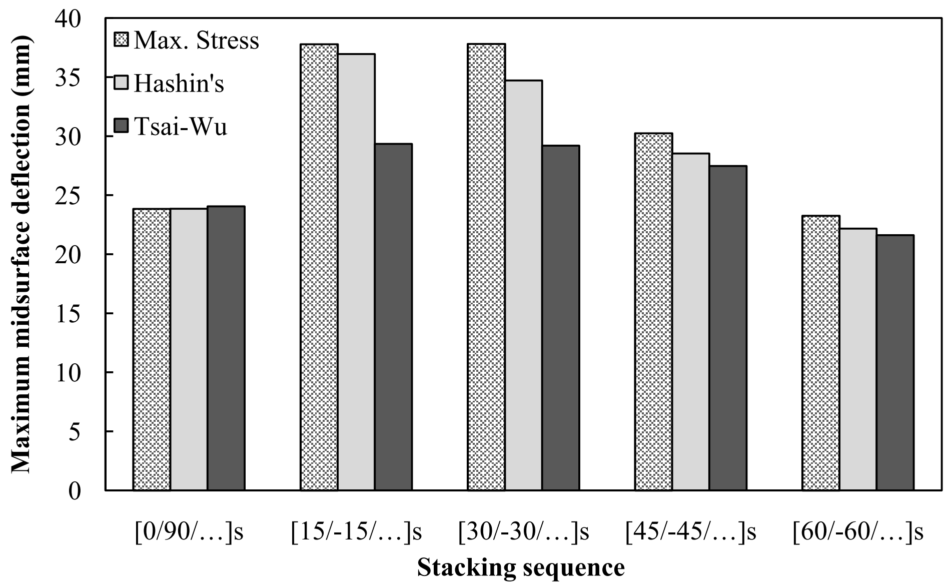

Figure 5: Maximum midsurface displacement at first ply failure for clamped roller plates

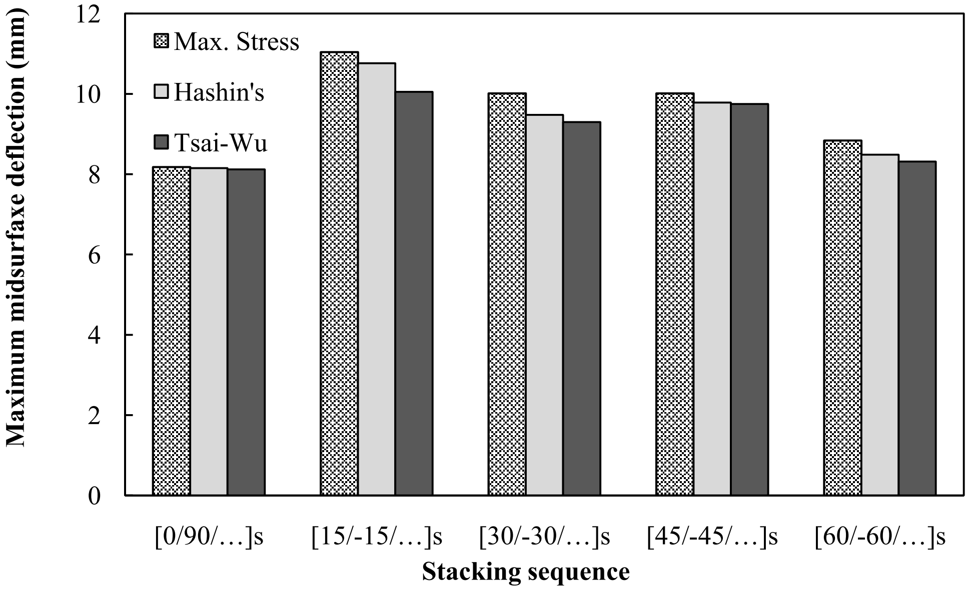

Figure 6: Maximum midsurface displacement at first ply failure for both ends clamped plates

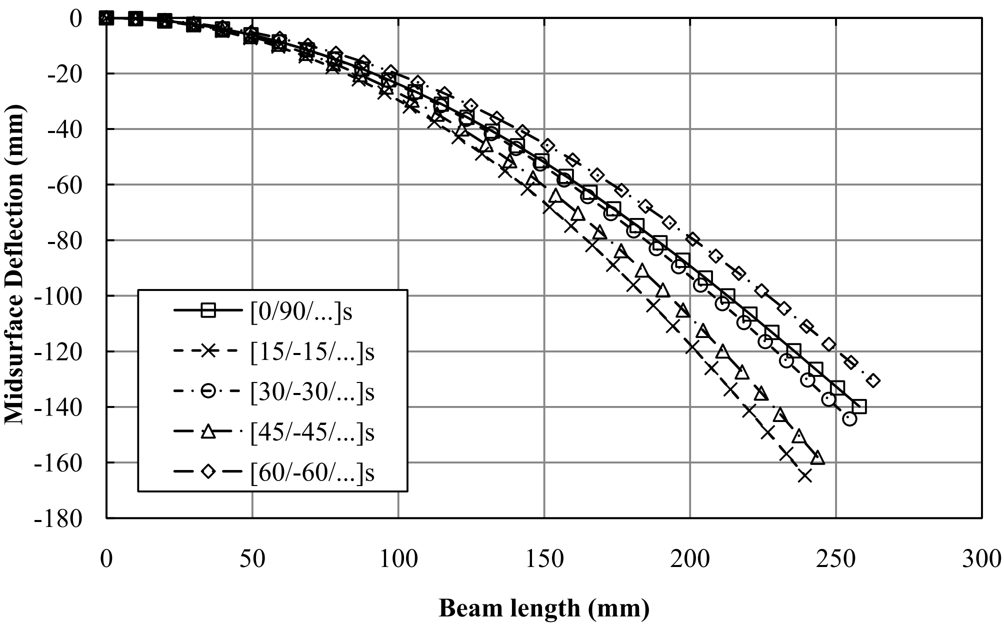

Figure 7: Deflection of one end clamped plates

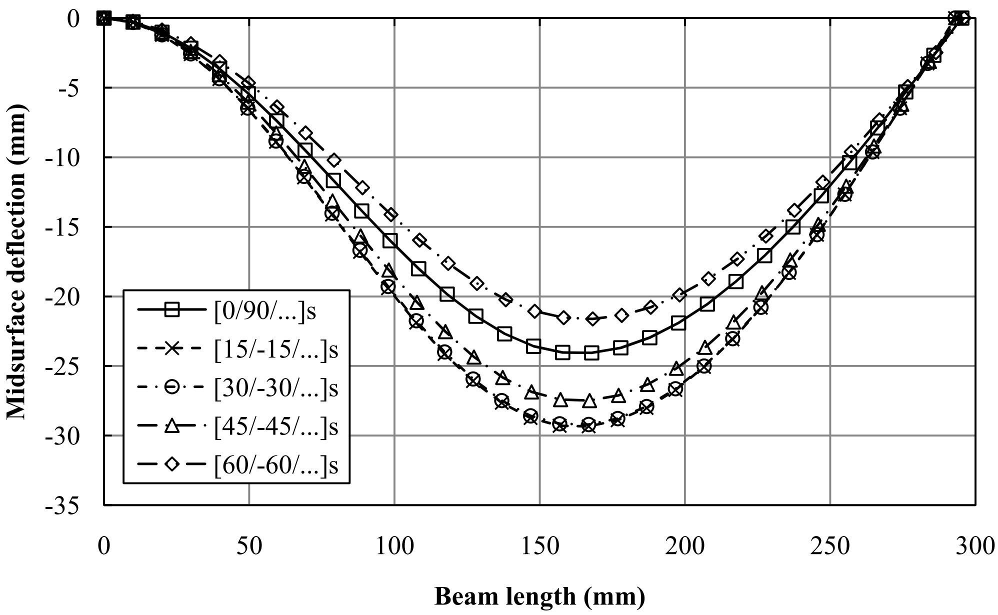

Figure 8: Deflection of clamped-roller plates

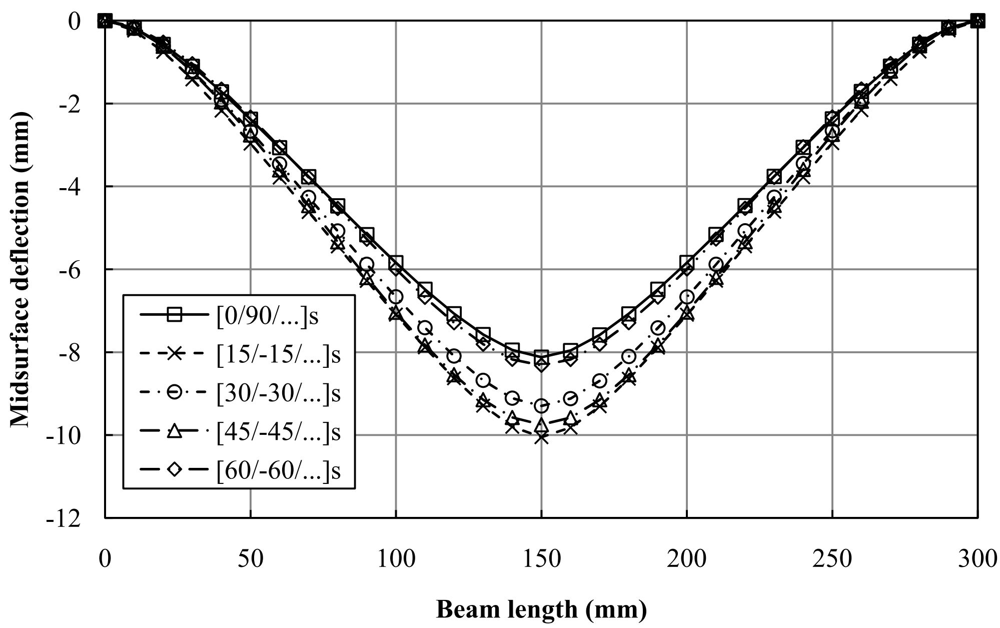

Figure 9: Deflection of both ends clamped plates

6 Conclusions

In the content of this study, the first ply failure and large displacement characteristics of the laminated flat composite plates made up of glass-epoxy composite are investigated through the use of the developed code. According to the current work, the following conclusions have been acquired:

1. The large displacements obtained to observe the first ply failure for all the cases analysed indicate that nonlinear deformation analysis is necessary for thin plates similar to those that have been considered in this study.
2. The results of the simulations showed that the first ply failure loads are found to be decreasing with increasing ply angles.
3. It is observed that the maximum stress criterion results in the highest first ply failure loads and the Tsai-Wu criterion yields the lowest first ply failure loads, whereas results of the Hashin's criterion lies in between.
4. It is found out that the displacements at first ply failure are decreasing with increasing ply angles for the same stacking sequence.
5. The maximum displacements are obtained from the maximum stress criterion, the minimum displacements are found from the Tsai Wu criterion, whereas the displacements obtained by the Hashin's criterion are in between.
6. A comparison for boundary conditions shows that as the boundary conditions get stiffer the first ply failure loads increase and the deflections experienced decrease.

References

[1] R. F. Gibson, "Principles of composite material mechanics", McGraw-Hill, 1994.

[2] M. M. Schwartz, "Composite Materials, Volume II: Processing, fabrication and applications", Prentice Hall, 1997.

[3] S. K. Mazumdar, "Composites manufacturing", CRC Press, 2001.

[4] M. M. Schwartz, "Composite materials handbook", McGraw-Hill, 1984.

[5] O. O. Ochoa, J. N. Reddy, "Finite Element Analysis of Composite Laminates", Kluwer Academic Publishers, 1992.

[6] G. S. Padhi, R. A. Shenoi, S. S. J. Moy, G. L. Hawkins, "Progressive failure and ultimate collapse of laminated composite plates in bending", Composite Structures, 40(3-4), 277-291, 1998.

[7] P. K. Parhi, S. K. Bhattacharyya, P. K. Sinha, "Failure analysis of multiple delaminated composite plates due to bending and impact", Bulletin of Materials Science, 24(2), 143-149, 2001.

[8] S. M. Spottswood, A. N. Palazotto, "Progressive failure analysis of a composite shell", Composite Structures, 53(1), 117-131, 2001.

[9] B. G. Prusty, S. K. Satsangi, C. Ray, "First ply failure analysis of laminated panels under transverse loading", Journal of Reinforced Plastics and Composites, 20(8), 671-684, 2001.

[10] W. P. Lin, H. T. Hu, “Nonlinear analysis of fiber reinforced laminates subjected to uniaxial tensile load”, Journal of Composite Materials, 36(12), 1481-1503, 2002.
[11] P. Pal, C. Ray, “Progressive failure analysis of laminated composite plates by finite element method”, Journal of Reinforced Plastics and Composites, 21(16), 1505-1513, 2002.
[12] P. Pal, S. K. Bhattacharyya, “Progressive failure analysis of cross-ply laminated composite plates by finite element method”, Journal of Reinforced Plastics and Composites, 26(5), 465-477, 2007.
[13] Z. M. Huang, “Failure analysis of laminated structures by FEM based on nonlinear constitutive relationships”, Composite Structures, 77(3), 270-279, 2007.
[14] H. Darendeliler, S. Oral, A. Turgut, “A pseudo-layered, elastic- plastic, flat-shell finite element”, Computer Methods in Applied Mechanics and Engineering, 174(1-2), 211-218, 1999.
[15] A. Tessler, T. J. Hughes, “A three node Mindlin plate element with improved transverse shear”, Computer Methods in Applied Mechanics and Engineering, 50, 71-101, 1985.
[16] J. Stegmann, “Analysis and optimization of laminated composite shell structures”, Ph.D. Thesis, Institute of Mechanical Engineering, Aalborg University, 2005.
[17] P. M. Wung, “Laminated composite structures by continuum-based shell elements with transverse deformation”, Computers and Structures, 62, 1073-1090, 1997.
[18] O. L. Roufaeil, T. Tran-Cong, “Finite strip elements for laminated composite plates with transverse shear strain discontinuities”, Composite Structures, 56, 249-258, 2002.
[19] G. T. Lim, J. N. Reddy, “On canonical bending relationships for plates”, International Journal of Solids and Structures, 40, 3039-3067, 2003.
[20] P. Malekzadeh, A. R. Setoodeh, “Large deformation analysis of moderately thick laminated plates on nonlinear elastic foundations by DQM”, Composite Structures, 80, 569-579, 2007.